Appl. Phys. B 82, 637–641 (2006)
DOI: 10.1007/s00340-005-2102-0

Applied Physics B
Lasers and Optics

S.-W. WANG[1,✉]
D. LIU[2]
B. LIN[2]
X. CHEN[1]
W. LU[1]

16 × 1 integrated filter array in the MIR region prepared by using a combinatorial etching technique

[1] National Laboratory for Infrared Physics, Shanghai Institute of Technical Physics, Chinese Academy of Sciences, Shanghai 200083, P.R. China
[2] Shanghai Institute of Technical Physics, Chinese Academy of Sciences, Shanghai 200083, P.R. China

Received: 31 August 2005/Revised version: 11 November 2005
Published online: 11 January 2006 •

ABSTRACT A combinatorial etching technique is introduced to prepare integrated narrow bandpass filters in the mid-infrared (MIR) region. In this region, a 16 × 1 filter array has been fabricated successfully with two deposition processes combined with the combinatorial etching technique. The pass bands of the 16 filter elements range from 2.534 to 2.859 μm with bandwidth ($BW_{3\,dB}$) less than 0.013 μm ($BW_{3\,dB}/\lambda \leq 0.48\%$). The insertion loss of the pass bands is between 1.75 and 3.43 dB. The results show that the technique is effective for the fabrication of filter arrays in the MIR region and can be extended to most of the important optical regions.

PACS 42.79.Ci; 84.30.Vn; 42.82.Cr; 42.82.Gw

1 Introduction

Optical filter arrays are one of the most important components in wavelength-division multiplexing (WDM) [1], multispectral devices [2] and parallel arrayed optics (including microlens arrays, microprism arrays, micromirrors and filter arrays) [3], which are widely used in communication systems and electro-optical systems. Traditionally, they can be mounted on a rotating wheel frame or employ tunable filters [4, 5] to realize the function of selecting the wavelength, but neither of these can obtain information in different bands simultaneously or be integrated in large numbers.

There are two types of filter arrays acquiring information simultaneously by controlling the optical thickness of the filter's spacer layer. One is with the pass band controlled by the refractive index of the spacer layer [6] and the other where it is controlled by the physical thickness of the spacer layer. For the former, it is only proposed theoretically and is very hard to be realized with large integration numbers. For the latter, it is realized in the form of wedge filters [2, 7] and is already commercially available. However, in a wedge filter it is not possible to have both a large dispersion (≫ 10 nm/mm) and a wide useful spectral region. Moreover, the dispersion will be limited by the wedge angle due to the non-parallel interface effect in the resonant cavity layer. Owing to these limitations, wedge filters are large (e.g. typical linearly variable filters in the 300–700 nm spectral range are 60 mm in length) and have a dispersion of about 5–10 nm/mm. Therefore, wedge filters can hardly be integrated with a large number of pass bands and are not suitable for the miniaturization of devices with existing technology [6].

The combinatorial etching technique [8–10] is a very highly efficient technique we developed to fabricate integrated filter arrays with narrow bandpass filters (NBPFs) on a single substrate. It can be applied in most of the important optical regions. In this paper, we demonstrate a 16 × 1 integrated filter array in the mid-infrared (MIR) region prepared by using such a technique.

2 Mechanism and fabrication procedure of the technique

We begin with a dielectric Fabry–Pérot-type filter; its schematic diagram and typical transmittance spectrum are shown in Fig. 1a and b, respectively. The transmittance of the structure can be expressed as follows:

$$T = T_0 / \left(1 + F \sin^2 \theta\right) . \tag{1}$$

Here T_0, F and θ can be expressed as

$$T_0 = T_1 T_2 / \left(1 - \sqrt{R_1 R_2}\right)^2 , \tag{2}$$

$$F = 4\sqrt{R_1 R_2} / \left(1 - \sqrt{R_1 R_2}\right)^2 , \tag{3}$$

$$\theta = (\varphi_1 + \varphi_2 - 2\delta)/2 , \tag{4}$$

where T_1, T_2, R_1, R_2, φ_1, φ_2 are the transmittance, reflectance and phase of the upper and lower mirror stacks, respectively, and δ is the phase thickness of the spacer layer.

Then, the maximum value of the pass band (center wavelength λ) will be

$$\lambda = \frac{2nd}{k + (\varphi_1 + \varphi_2)/2\pi} = \frac{2nd}{m} , \tag{5}$$

where $m = k + (\varphi_1 + \varphi_2)/2\pi$, $k = 0, 1, 2, \ldots$.

Equation (5) indicates that the pass band of the filter is decided by the optical thickness (nd) of the spacer layer. It is proportional to the thickness (d) of the spacer layer with

✉ Fax: +86-21-65830734, E-mail: wangshw@mail.sitp.ac.cn

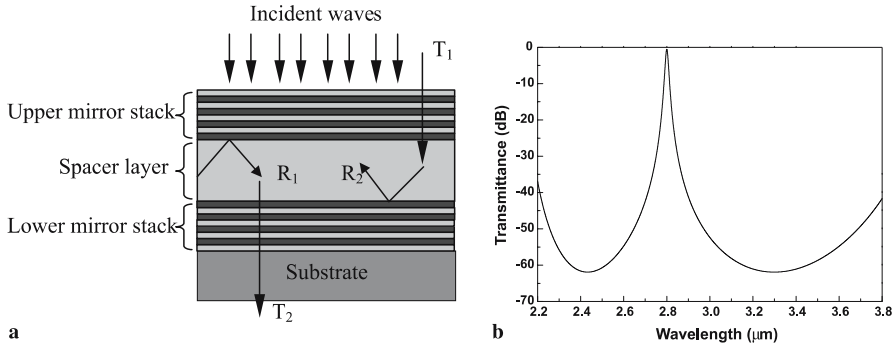

FIGURE 1 (**a**) and (**b**) Schematic diagrams of a dielectric Fabry–Pérot-type filter and its typical transmittance spectrum

a constant refractive index (n). A series of filters with different pass bands can be obtained just by changing the thickness of the spacer layer. Then, they can be integrated on a single substrate easily if a series of spacer layers with different thicknesses can be fabricated. The difficulty in fabricating a filter array focuses on the realization of spacer arrays with different thicknesses. It can be readily overcome by using the combinatorial etching technique, which produces 2^N different thicknesses of spacers with only N etching processes.

Figure 2 shows the procedure diagram for the fabrication of a filter array by the combinatorial etching technique. A filter array with 2^N elements needs only N combinatorial etching processes and two deposition processes. Firstly, the lower mirror stack and the spacer layer are deposited on the substrate as shown in Fig. 2a. Then, the spacer layer is etched to be an array with different thickness by the combinatorial etching technique (see Fig. 2b–d). During the combinatorial etching processes, a series of masks are used to realize the function of selective etching on different areas of the spacer layer. The window's shape and size of the mask, corresponding to the shape and size of the filter array, can be designed to match the detector array. The mask is valid for filter sizes in centimeters or millimeters. Photolithography can be utilized for smaller filter sizes. The total etching thickness (or, in other words, the residual thickness of the spacer) of each area is different from the others, which will lead to the pass-band difference in different areas. After depositing the upper mirror stack onto the resultant structure, a filter array with a series of distinct pass bands is completed as shown in Fig. 2e. Its three-dimensional (3D) schematic diagram is shown in Fig. 2f.

3 Results and discussion

Unlike traditional filter-fabrication techniques, our method involves two deposition and N etching processes. Their effects on the property of the fabricated filters should be taken into account. The feasibility analysis of the combinatorial etching technique is presented elsewhere [9]. The results show that it is a good way to combine the deposition and etching processes for fabrication of a filter array, and a 32×1 filter array in the visible–near-infrared region has been fabricated by the combinatorial etching technique [9].

For filters in the MIR region, Ge and SiO are chosen as high and low refractive index materials with n_{H} and n_{L} of 4.05 and 1.75, respectively. Since the absorption of the spacer layer is vital to the property of Fabry–Pérot-type filters, the relatively low absorption material SiO in the MIR region is selected as the spacer layer. Then, the etching process is conducted on the material SiO with a dry etching method of an ion-beam etching machine (LKJ-1C, home made). The thickness of the spacer layer is controlled by the etching rate of SiO. In order to control it as precisely as possible, corresponding to the control of the filter's pass band, a series of samples with the same original thickness of SiO have been etched with differ-

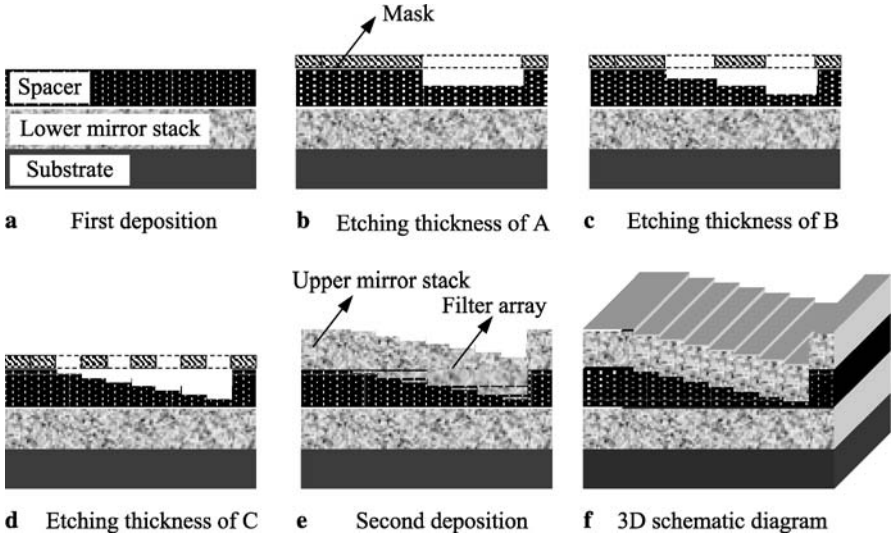

FIGURE 2 Procedure diagram for the fabrication of a filter array by using the combinatorial etching technique, where (**a**) is the first deposition for lower mirror stack and spacer layer. (**b**)–(**d**) are the combinatorial etching processes. (**e**) is the second deposition for upper mirror stack. (**f**) is the 3D schematic diagram of the fabricated filter array

ent times from 10 min to 80 min. The resultant thicknesses of the samples are obtained by fitting their transmittance spectra and a sample without having been etched is compared as a reference. The etching thicknesses of each sample with different etching times are presented in Fig. 3. From the figure, we can see that the etching thickness is almost linearly changed with the etching time in a large range. The line is the fitting result with these experimental data. The results show that the etching rate of SiO is 14.86 nm/min, corresponding to 0.25 nm/s. Therefore, the controlled precision of the thickness of SiO should also be in this order.

The original filter is designed to be $(1L1H)_4 2.0L (1H1L)_4$ with design wavelength λ_0 of 2.800 μm, where H and L are $\lambda_0/(4n_H)$ and $\lambda_0/(4n_L)$, respectively. The center wavelength λ of the pass band is mainly determined by the optical thickness of the spacer layer and can be adjusted by varying its thickness for the selected material (the refractive index is constant). The control of the thickness of the spacer layer can utilize the etching process as mentioned above. During the first deposition, the lower mirror stack of $(1L1H)_4$ and the spacer layer of 2.0L are deposited on the substrate of double-polished silicon by using electron-beam evaporation and their thicknesses are controlled by an optical monitor. Then, the spacer layer has been produced to be a 16 × 1 spacer array with thickness discretely distributed in the range of 2.0–1.4L, corresponding to thickness distributed from 800 nm to 560 nm, realized by only four etching processes. The size of each element is 0.74 mm × 12 mm. The resultant structures act as some kind of mirror stacks. Figure 4 shows the picture of this half-made sample after four combinatorial etching processes. Fifteen areas in different colors in the center region of the sample represent 15 areas of the spacer layer of different thicknesses. The 16th area of the spacer is the same as the background, since it has not been etched. These areas correspond to the areas of the filter array in the final structure. A 16 × 1 filter array has been completed after depositing the upper mirror stack of $(1H1L)_4$ on the above structure as shown in Fig. 4.

The corresponding spectra of each filter element and their insertion loss are shown in Fig. 5 measured by using a Fourier transform infrared (FTIR) spectrometer (Perkin Elmer Instruments). The pass bands of the 16 filter elements range from 2.341 to 2.770 μm. They are distributed almost linearly except for filters 8 and 9. The bandwidth ($BW_{3\,dB}$, at 3 dB down from the peak) of the pass bands is between 0.004 and 0.015 μm (corresponding to $BW_{3\,dB}/\lambda$ of 0.15–0.53%), indicating that all the filters integrated on the substrate are ultra-NBPFs. The insertion losses of the pass bands range from 8.98 to 15.5 dB. Most of them are less than or near 11 dB. Since the filters integrated on the array are ultra-NBPFs, they are very sensitive to the fabrication conditions and processes, such as deposition control precision, absorption of the materials, scattering loss, etching and the two deposition processes. In this case, they are vital to the property of the pass bands and are the main reasons for the large insertion loss. The insertion loss should be smaller for filter arrays with wider pass bands, which can be realized by reducing the number of (LH) pairs of the filters. Figure 6 shows the transmittance spectra and their insertion loss of a 16 × 1 filter array with three (LH) pairs, corresponding to a structure of $(1L1H)_3 xL (1H1L)_3$. The pass bands of the 16 filter elements range from 2.534 to 2.859 μm. They are distributed more uniformly than those of a filter array with four (LH) pairs. The results show that the property of the filter array is much better than that of the filter array with four (LH) pairs as shown in Fig. 5. The insertion loss of each filter element is no more than 3.43 dB and the lowest one comes to 1.75 dB, which is much smaller than that of the filter array with four (LH) pairs. The bandwidth of the pass bands is between 0.009 and 0.013 μm and the relative bandwidth of $BW_{3\,dB}/\lambda$ ranges from 0.32 to 0.48%. They are also ultra-NBPFs.

To investigate the polarization dependence of the filter arrays, the samples with four (LH) pairs are measured under *s*- and *p*-polarizations by using a Lambda 900 spectrophotometer (200–2500 nm). The *s*- and *p*-polarized transmittance spectra from filter 1 to filter 6 (confined by the range of the spectrophotometer) are measured and presented in Fig. 7, where the *s*- and *p*-polarized spectra are indicated by the solid line and the dotted line, respectively. The *s*-polarization curve

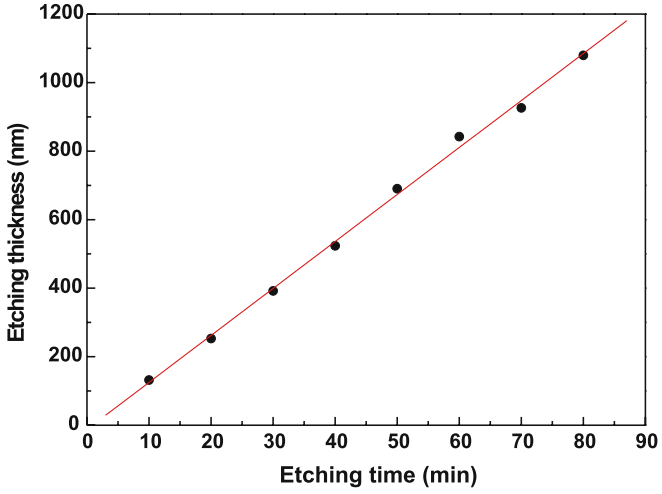

FIGURE 3 The change of etching thickness of SiO with etching time. The *line* is the fitting result with the experimental data

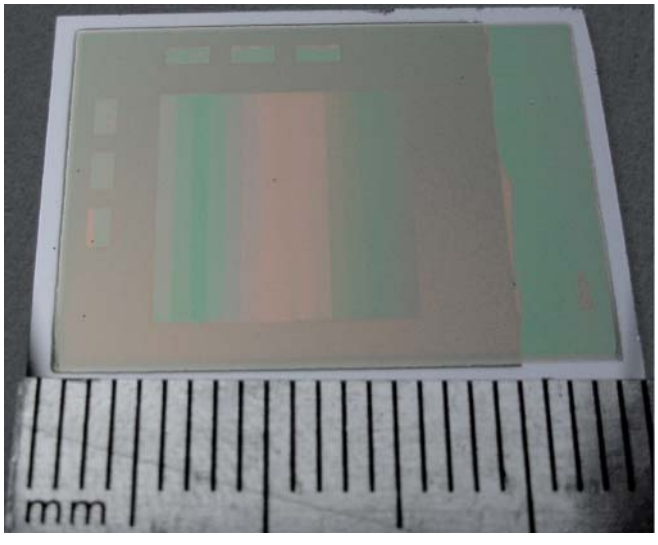

FIGURE 4 The picture of the half-made sample after four combinatorial etching processes

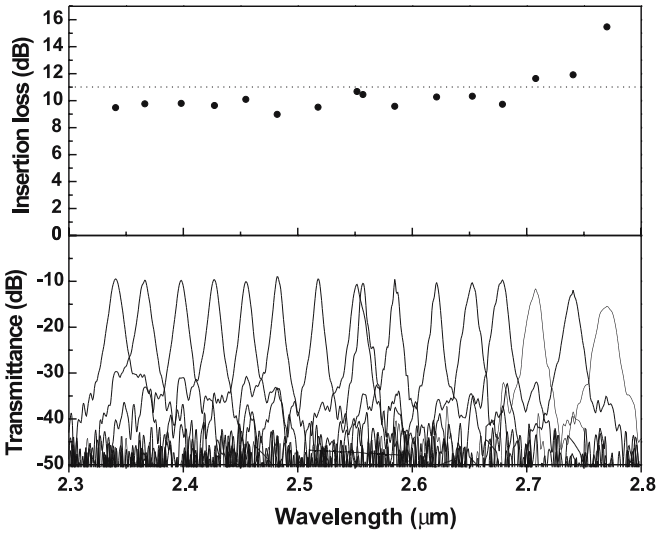

FIGURE 5 Transmittance spectra and insertion loss of each element on the 16×1 filter array, with element size of 0.37 mm × 12 mm. The filter structure is $(1L1H)_4 x L(1H1L)_4$ with design wavelength λ_0 of 2.800 μm, $x = 2.0$–1.4, where H and L are the thicknesses of the high and low refractive index materials Ge and SiO with $n_H = 4.05$ and $n_L = 1.75$

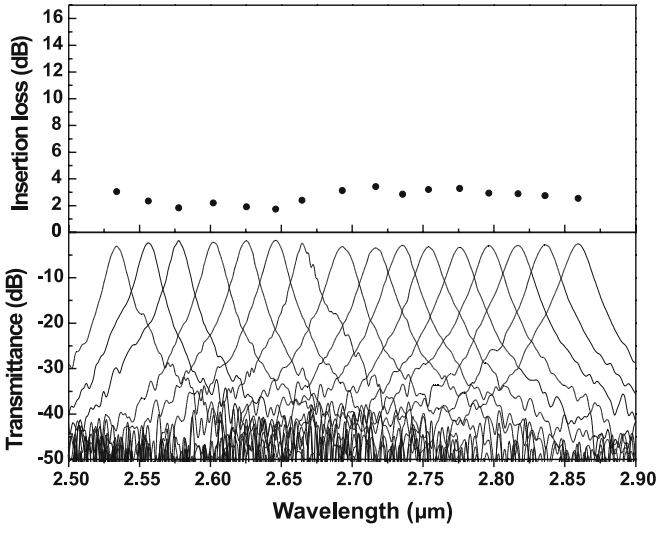

FIGURE 6 Transmittance spectra and insertion loss of each element on the 16×1 filter array with three (LH) pairs. The filter structure is $(1L1H)_3 x L(1H1L)_3$ with design wavelength λ_0 of 2.800 μm, where H and L are the thicknesses of the high and low refractive index materials Ge and SiO with $n_H = 4.05$ and $n_L = 1.75$

overlaps with the *p*-polarization curve well for all the filter elements measured. The results show that the filter arrays fabricated by the combinatorial etching technique are polarization independent and the etching processes will not result in a polarization problem.

Actually, a similar structure integrated with 32 NBPFs has already been fabricated successfully with a filter size of 0.37 mm × 12 mm. Filter arrays with larger integration numbers can also be easily fabricated by using the combinatorial etching technique. However, the size of the filters is too small to be measured with a regular FTIR spectrometer. The transmittance property of the filters may be obtained with a micro-FTIR spectrometer. Two-dimensional (2D) filter arrays in the MIR region can also be fabricated just by repeating the etching processes on the other dimension. The filter array fabricated by our technique can be readily designed to match with a one-dimensional or 2D photodetector array and form a compact spectrophotometer. The results in this paper show that the combinatorial etching technique is also effective for fabricating filter arrays in the MIR region and can be extended to most of the important optical regions. The filter arrays realized by such a simple technique can not only match the demand of multispectral acquisition systems and parallel arrayed optics, but also can be used in flat-panel color displays, sensors and so on.

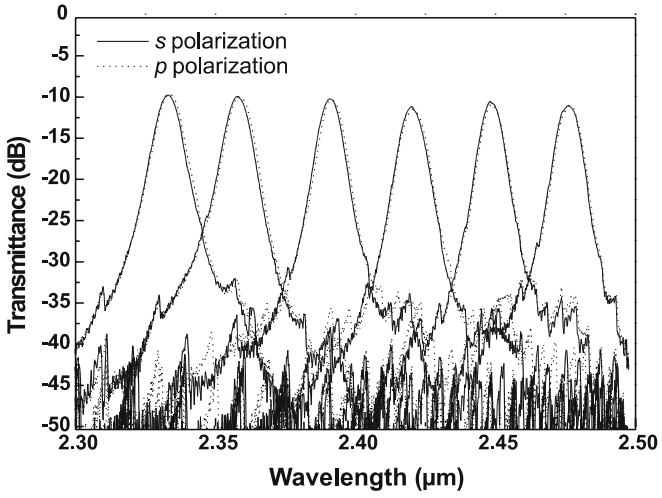

FIGURE 7 *s*- and *p*-polarized transmittance spectra of the filter array with four (LH) pairs, indicated by the *solid line* and the *dotted line*, respectively. The filter structure is $(1L1H)_4 x L(1H1L)_4$

4 Conclusion

In this paper, we introduced the mechanism and fabrication procedure of the combinatorial etching technique for the integration of NBPFs. A 16×1 filter array in the MIR region has been fabricated successfully with only four combinatorial etching processes. The pass bands of the elements range from 2.534 to 2.859 μm with bandwidth less than 0.013 μm ($BW_{3\,dB}/\lambda \leq 0.48\%$). The insertion loss of the pass bands ranges from 1.75 to 3.43 dB. It is much harder to fabricate a filter array integrated with ultra-NBPFs with narrower designed bandwidth. The filter arrays fabricated by the combinatorial etching technique are polarization independent. The results show that the technique is effective for the fabrication of filter arrays in the MIR region and can be extended to most of the important optical regions. Such a NBPF array can be used in many optical applications.

ACKNOWLEDGEMENTS This work is sponsored by the Shanghai Rising-Star Program (05QMX1459) and the National Natural Science Foundation of China (60508018). The authors thank Ms. Daqi Li in the Institute for the measurements of polarized transmittance spectra.

REFERENCES

1 M. Aziz, P. Meissner, T. Hermes, Opt. Commun. **208**, 61 (2002)
2 D. Hunkel, M. Marso, R. Butz, R. Arens-Fischer, H. Lüth, Mater. Sci. Eng. B **69–70**, 100 (2000)
3 M. Frank, B. Schallenberg, N. Kaiser, Opt. Eng. **36**, 1220 (1997)

4 L. Bei, G.I. Dennis, H.M. Miller, T.W. Spaine, J.W. Carnahan, Prog. Quantum Electron. **28**, 67 (2004)
5 D. Hohlfeld, M. Epmeier, H. Zappe, Proc. SPIE **4989**, 143 (2003)
6 S. Kaushik, B.R. Stallard, Proc. SPIE **2532**, 276 (1995)
7 Z. Jaksic, R. Petrovic, D. Randjelovic, T. Dankovic, Z. Djuric, W. Ehrfeld, A. Schmidt, K. Hecker, Proc. SPIE **3680**, 611 (1999)
8 S.-W. Wang, D. Liu, B. Lin, X. Chen, Z. Li, Y. Shi, W. Wang, W. Lu, Int. J. Infrared Millim. Waves **25**, 1677 (2004)
9 S.-W. Wang, L. Wang, Y. Wu, Z. Wang, X. Chen, W. Lu, Opt. Lett. **31**(3) (2006)
10 S.-W. Wang, L. Wang, Y. Wu, Z. Wang, D. Liu, B. Lin, X. Chen, W. Lu, Acta Opt. Sin. **26**(6) (2006) (in Chinese)